UNIVERSITE KASDI MERBAH OUARGLA

Faculté des Mathématiques et des Sciences de la Matière

Département de Physique

Mémoire

MASTER ACADEMIQUE

Domaine : Science de la Matière

Filière: Physique

Spécialité: Physique des Matériaux

Présenté par : CHAOUCHE Latifa

Thème

ELECTRON PARAMAGNETIC RESONANCE AND MAGNETIC SUSCEPTIBILITY IN THE CuCrZrSe4 SPINEL COMPOUND

Soutenu publiquement

Le:…/05/2016

Devant le jury :

Mr. R. GHERIANI	**MCA**	**Président**	**UKM Ouargla**
Mme. K. BELAKROUM	**MCA**	**Encadreur/rapporteur**	**UKM Ouargla**
Mr. O. BOUKRAA	**MCB**	**Examinateur**	**UKM Ouargla**

Année Universitaire : 2015/2016

Acknowledgements

First We thank our god who gaves us the strength to complete this modest work.

I would like to express my deepest gratitude to Dr Karima BELAKROUM, not only for giving me the opportunity to write this thesis but also for her support and her numerous suggestions were extremely helpful to complete this thesis.

I will not forgot to thank , Dr. Rachid GHARIAN and Dr.Omar BENTOUILA for agreeing to participate in the jury.

I thank all my colleagues at the University and department of physics, specialy Material physics (2015-2016)

Finally, I am forever indebted to my parents, brother and sisters for their endless patience and encouragement when it was most required. I am very grateful for their support.

Summary

General introduction

A frustrating situation can be generated by a particular geometry of distribution of atoms carriers of magnetic moments, or in insulating compounds semiconductors. This is a topological frustration with a well-known illustration is provided by the triangular antiferromagnetic Ising or cubic face-centered lattice. In the example of less academic EuxSr1-xS, frustration comes from the existence simultaneous interactions of short types: between ferromagnetic first neighbors Eu^{++}, and antiferromagnetic between second neighbors. The juxtaposition of frustration and disorder leads to a spin-glass behavior, which is the case of the title compound above. These problems arouse great interest among theorists. However, it should recognize that there is a lack of new materials that can enrich experimentation whose theory feeds. The current state of efforts to understand the phenomenon of geometric magnetic frustration is described in the context of several materials. Spinels having transition metal ions on the plots A octahedral and tetrahedral B often have interesting magnetic properties, may reflect the presence of frustration for some types of magnetic interactions. It is known that, if a carrier of time does not occupy all the octahedral sites a spinel structure, the particular geometry of the subnetwork B of these sites may result a frustration level interactions when they are negative. Considerations this theoretical time, conducted about a new type of magnetic arrangement observed in some alloys, gave a renewed interest in compounds with this structure. In this area of investigation where theory precedes experience now, it seems interesting to provide compounds have characteristics would be close to ideal models. The system is formulated My ^{I}M $^{III}M_yM^{IV}{}_{2-y}S_4$ (M^{I} = Cu, M^{III} = Cr, M^{IV} = Sn) where sites octahedral welcomed pairs of diamagnetic elements. These compounds magnetically diluted system properties. The magnetic behavior chrome samples is explained by considering the presence of finite clustersCr^{3+} , and Cr^{3+} existing isolated paramagnetic. The system had all likely to be characterized for obtaining insulating spin glasses.

In order to understand, the role of the interactions intensity. We sought to accentuate their antiferromagnetic character involving chromium-chromium shorter distances. This was achieved using a diluted element size smaller than that of tin IV. Our choice fell on zirconium, which led to the study of the $CuCrZrSe_4$ system. The $Cu^{I}Cr^{III}Zr^{IV}Se_4$ phases are entirely original, the consequences of dilution, would then everything other than those envisaged for$Cu_y{}^{I}Cr_y{}^{III}Zr_{2-y}$ $^{IV}Se_4$ systems. Indeed, when the dilution is carried out in an

orderly fashion, some interactions near neighbors disappear into the referral network. Chromium III was chosen because the absence of orbital angular momentum, due to its fundamental term $^4A_{2g}$ in octahedral site. The expected magnetic interactions will therefore isotropic Heisenberg type, as they result from the only contribution of spin. We were interested in studying the magnetic properties of $CuCrZrSe_4$ compounds by measurements of magnetic susceptibilities, and magnetization hysteresis loop with the magnetometer SQUID Quantum Design- MPMS-5S.As well as measures to alternative susceptibility From an experimental standpoint, these susceptibility measurements alternating field are indicative of the presence of a spin glass transition. Indeed, when applying a sinusoidal field with a certain frequency, the response magnetic material is also sinusoidal, the same frequency, but it is more shifted the time relaxation of the system is large. Thus, in the glass phase spin, the real part of the susceptibility is even lower than the frequency is high; a displacement towards higher temperatures was observed for the maximum of the curve $\chi = f(T)$ and use of measures Electron Paramagnetic Resonance Spectroscopy (E.P.R). Electron spin resonance (ESR) spectroscopy is certainly one of the most powerful tools to investigate the magnetic properties of the frustrated systems. ESR is a major probe not only to investigate the paramagnetic state of these materials but also to probe these materials at low temperatures.

In this Thesis, a study of magnetic properties of CuCrZrSe4 compound, In the first chapter we introduce the concepts and theoretical knowledge concerning the geometric frustration in a magnetic system, and describe several experimental realizations. We will show include experimental features spin glasses which remain a field of major scientific debate This thesis is divided to three chapters as follow:

Chapter 1, the physics of order and broken symmetry in low-dimensional magnets is explained. Some theoretical models are discussed.

Chapter 2, the experimental technique (ESR) used in this work is introduced.

Chapter 3, the detailed ESR and SQUID measurements and analysis of powder CuCrZrSe4 are reported.

Chapter 01

Frustration and magnetic behavior in the spinel system

In this chapter, we present some general magnetic properties of spinel systems, where we describe the magnetic couplings of super exchange, the origin of the order of ferrimagnetic spinel oxides, and we specifically describe the diluted magnetic semiconductors and ferromagnetic semiconductors. Here we give the basics about the frustrated systems without disorder in which frustration, unlike the spin glasses, comes not from the disorder but the particular network topology. This is called "geometrical frustration" as opposed to frustration induced disorder. These systems have become very popular recently because of the wealth of behaviors they exhibit low temperature. Finally, we review the various experimental characteristics of spin glasses.

1-Magnetic properties of spinel

Ferromagnetic ceramics, which originally were designed specifically to avoid losses that occur at high frequencies in the conventional ferromagnetic materials, are mixed iron spinels and various other metal oxides. Spinel ferrites have properties quite similar to those of ferromagnetic: one of them, moreover, magnetite, was the first known ferromagnetic and gave its name to the phenomenon of magnetism. Several magnetic oxides of commercial importance have the spinel structure. Systems with spinel structure are more interesting because they provide the opportunity to present a wide variety of magnetic disorder and frustration in the system [1,2,3,4].

Several studies have shown that inorganic compounds with spinel structure AB_2X_4, have fascinated physicists for many years, because the topology of their network site B (tetrahedral site) trend frustrates the load and spin order. Chalcogenides with spinel structure AB_2X_4 (X is O, S, Se, or Cl) have been extensively studied for their various physical properties in recent decades, they show a great variety of interesting ground states, including superconductivity, the cooperative antiferromagnetism, heavy fermion and the charging order. The range of different properties exhibited by spinels results from the effect of Coulomb interactions, of frustrated magnetization effects, and the electron-lattice interaction. The tetrahedral network locations B in the spinel structure can adopt a large number of charge

ordering model. The tetrahedral network in the spinel structure causes geometrical frustration when the ions occupying the B sites are magnetic. Electronic and magnetic states made in a complex environment are often multi-degenerate and fluctuate. Because of these complexities, a number of properties of spinel remain poorly understood. Spinels are therefore important topics of research in the physics of strongly correlated materials. Certain compounds, such as lithium manganese spinel having the structure used in the cathodes of battery and in microwave applications are of substantial technological importance. Topics concerning transition metal oxide spinel are part of a dual theme:

- The electrochemical energy storage in the form via lithium batteries,
- The magnetic frustration in spinel is a remarkable example.

  The Li-Mn-O system: recent studies were:
- The influence of substitutions and the presence of gaps in the intercalation and magnetism.
- The presence of cation order or superstructures for special rate of intercalation (case Li0.5Mn2O4).
- Electrochemical structure-property relations

Thus, the spinel ferrite is very important magnetic oxides of technologically because of their magnetic and electrical properties (high resistivity, low eddy current and dielectric loss). Ferrites are extensively used in microwave devices, computers, magnetic recording media, etc.. Knowing the distribution of cations and spin alignment is essential to understanding the magnetic properties of spinel ferrite. The interesting physical and chemical properties of ferro-spinel result from their ability to distribute cations among the tetrahedral sites (A) and octahedral (B) available. Cobalt ferrite has an inverse spinel structure and the degree of inversion is dependent on the heat treatment. Much work show that the addition of the tetravalent ions Si4 +, Ge4 + and Ti4 + in cobalt ferrite causes influences on the structural, electrical and magnetic. The ion substitution of Cr3 + is likely to increase the resistivity and reduce the saturation magnetization. The addition of the tetravalent ions Sn4 +, Ti4 + in the spinel ferrite can also influence the electrical and magnetic properties. A weak ion substitution Sn 4+ ferrite can lead to increase in resistivity and consequently to reduce the dielectric properties. To demonstrate the substitution effect Cr3 + in the presence of a little Sn 4+ cobalt ferrite, studies on ferrite$Co_{1+\ y}Sn_yFe_{2-2y-x}Cr_xO_4$ are undertaken. The sulfochromites $ZnCr_{2-2x}In_{2x}S_4$ are compounds spinel structure, the space group is Fd 3 m. For x = 0, the spinel structure is the type normal, the tetrahedral sites are occupied by the zinc atoms and

octahedral sites are occupied by atoms of chromium. When the cationic distribution reversed a the inverse spinel configuration is obtained [5,6,7]. Another study was carried out on the $Cu_{1-x}Zn_xIr_2S_4$ system ($0 < x < 0.9$) by X-ray diffraction, electric resistivity and measures magnetic susceptibility. The compound being CuIr2S4 metal temperature ambient, undergoes structural transition phase to a lower symmetry around230K and becomes a low-temperature insulation. The substitution Zn Cu allowed essentially remove the metal-insulator transition, resulting in an impact on thesuperconductivity.

1.1-Couplings AB, BB and AA

The magnetic couplings in the spinel oxides are super kind exchange. The super exchange coupling of the relay is the anion O^{2-}. The sign and strength of coupling between two ions depend hybrid cation states with the states of the anion and the number of electrons in the 3d shell according to empirical rules Goodenough-Kanamori [8,9] . Accordingly, the intensity of coupling depends on the nature of the two cations, but also the length and angle of the Me-O-Me bonds. More it is close to 180, the more coupling is strong. More links are long unless the coupling is strong. The order magnetic result of the ferromagnetic or antiferromagnetic nature and the intensity of super cation exchange couplings between sites A and site B (coupling A-B) between A cation sites (coupling A-A) and cation between sites B (coupling B-B). Both the most important couplings are couplings A-B (always antiferromagnetic) and B-B (Most often antiferromagnetic) between first neighbors.

1.2-Collinear ferrimagnetism

The exchange interactions are characterized by the exchange constants Jij in using a Hamiltonian isotropic Heisenberg exchange between neighboring cations i and j :

$$H = -2 Jij Si Sj$$

With this sign convention, $Jij > 0$ for a ferromagnetic coupling. Most of the time, the saturation magnetization of the resulting magnetic coupling majority antiferromagnetic cations between subnets A and B. When the orbital part of the magnetic moment of the cation is negligible, the magnetization per formula unit can be estimated easily [10]. For example, Fe^{3+} ions have a spin S = 5/2 and a fundamental condition not orbitally degenerate (^{6}A1g (Oh)). By neglecting the orbital part, their atomic magnetic moment is m (Fe^{3+}) = g <S> = uB 5μB.

To form the group (Fe^{3+}) A [$Fe^{3}{}_{5/3}$] BO^{4} . The experimental values are determined from 3.15 to 3.17μB. When the atomic moments are perfectly aligned parallel or antiparallel, it is called Neel collinear ferrimagnetism. The ferrimagnetic order disappears above the Curie temperature.

1.3-Effect of the magnetic dilution

The magnetic order is more complex when a subnet is fully occupied by a diamagnetic ion. For zinc ferrite (Zn^{2+}) A [$Fe^{3+}{}_{2}$] BO4, the dominant antiferromagnetic interaction A-B is absent, since the Zn^{2+} ion is diamagnetic (3d10). The coupling B-B also is antiferromagnetic. But the observed order is a complex non-collinear antiferromagnetic order with a Neel temperature of 10K [9]. The Neel temperature is the temperature above which antiferromagnetic order disappears. In addition, the magnetic order is very dependent on the nature of the diamagnetic ion occupying one of the two subnets. It is likely that there are long-range interactions involving the diamagnetic ion: A-O-B-O-A or B-O-A-O-B according to the diamagnetic ion occupies the subnet B or A. In the case of a diamagnetic subnet A, there is a small reversal of the diamagnetic ion, the antiferromagnetic coupling antiferromagnetic AB disturbs the arrangement of the network of sites B. It appears a local order in the vicinity of some cations paramagnetic present on the subnet A. Locally, network cations have a ferromagnetic order them. This happens for (Zn^{2+}) A [$Fe^{3+}{}_{2}$] BO_4, spinel for which the inversion depends on the method of synthesis of the material. When a subnet is partially occupied by diamagnetic ions, the situation is also complicated and the magnetic order eventually deviate from the collinear ferrimagnetism [11,12,13]. This is the case of zinc and nickel ferrites, of formula ($Fe^{3+}{}_{1-\delta}Zn^{2+}{}_{\delta}$)A($Fe^{3+}{}_{1+\delta}Ni^{2+}{}_{1-\delta}$)$BO_4$. When the ion substitution rate Zn^{2+} (δ) increases, at first the magnetization increases in accordance with a collinear ferrimagnetism model. Moments subnet B ions are less and less compensated by the antiferromagnetic coupling with the moments of ions subnet A. However, from a certain value of δ (δ = 0.5), the magnetization begins to decrease when δ increases. In fact, the number of ions Fe^{3+} A decrease, there is competition between exchanges antiferromagnetic AB and BB, one designed to impose a ferromagnetic order between the times of the subnet B, the other tending to impose antiferromagnetic order on the subnet B. It appears a canting of the spins on the subnetworks a and B, called "Yafet-Kittell." For a large magnetic dilution (δ> 0.8), the long-range magnetic order concerns only the subnet B, which decouples two

magnetic subnets antiferromagnetically coupled. "The magnetic dilution" results in different types of magnetic order in short or long distance, including "spin glass" state.

1.4-Diluted magnetic semiconductor and ferromagnetic semiconductor

The terminology for semiconductors having a magnetic phase (ferromagnetism, antiferromagnetism, spin glass state, ...) has evolved over time. The terms of diluted magnetic semiconductor (DMS for Diluted Magnetic Semiconductor) or semi magnetic semiconductor were employed from the sixties when these semiconductors had a spin glass magnetic phase. The term "ferromagnetic semiconductor" appeared in the early 90's when advances in processing techniques have helped to incorporate a larger amount of magnetic elements in III-V semiconductors, and from the time where these semiconductors exhibited a clearly defined ferromagnetic phase.

The magnetic semiconductor can be divided into two distinct families:

- Semi-conducteurs où les éléments magnétiques forment un réseau périodique, EuS, $CdCr_2Se_4$ par exemple
- Semiconductors where the magnetic elements randomly replace the Cd1-xMnxTe cations, for example $Ga_{1-x}Mn_xAs$.

Different semiconductors where the magnetic elements of families form a periodic network are for example chalcogenides based on chromium or europium and manganites.

cation) and ferromagnetic (cation-cation). Manganites can be also presented as magnetic semiconductors. The ferromagnetic order of these compounds in the competition between the ferromagnetic double exchange interaction and the antiferromagnetic interaction of super exchange [14,15].

The geometrically frustrated systems have been the subject of numerous theoretical studies, but are experiencing a renewed interest since the discovery of new experimental achievements in the early 90. One of these achievements is the $SrCr_{9p}Ga_{12-9p}O_{19}$ compound, potential candidate liquid physics spins, and the center of experimental studies in this field. A magnetic system consists of a regularly distributed sites network or not interacting. A system is frustrated if the interactions between sites are contradictory [16,17]. There are two classes of frustrated magnetic systems.

- Spin glasses where disorder induced frustration.

- The geometrically frustrated magnetic systems in which frustration is generated by the network geometry, without the presence of disorder.
-

1.5-Geometrical frustration

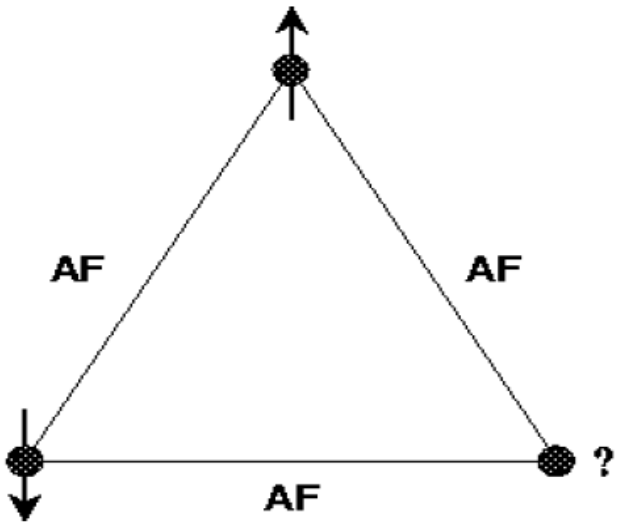

Fig.1.1: Example of geometrically frustrated system: the triangular lattice with antiferromagnetic interactions [18].

A system is geometrically frustrated if frustration comes from the geometry or the network or interactions. One example of completely frustrated by network geometry system is that of triangular lattice with antiferromagnetic interactions shown in Fig.1.1. It has in this case not messy at all, nor in the positions of spins (they are all placed at the sites of a regular lattice), or in the signs of couplings (the interactions are all of the same sign).

An example of the same order to illustrate this time a frustration induced by the geometry of the interaction is that of fig.1.2. This is a square array with ferromagnetic coupling between nearest neighbors J1, and J2 between antiferromagnetic second neighbors (along the diagonals of the squares). If | J1 | = | J2 |. The system is frustrated and elementary plate, at least two links can not be satisfied.

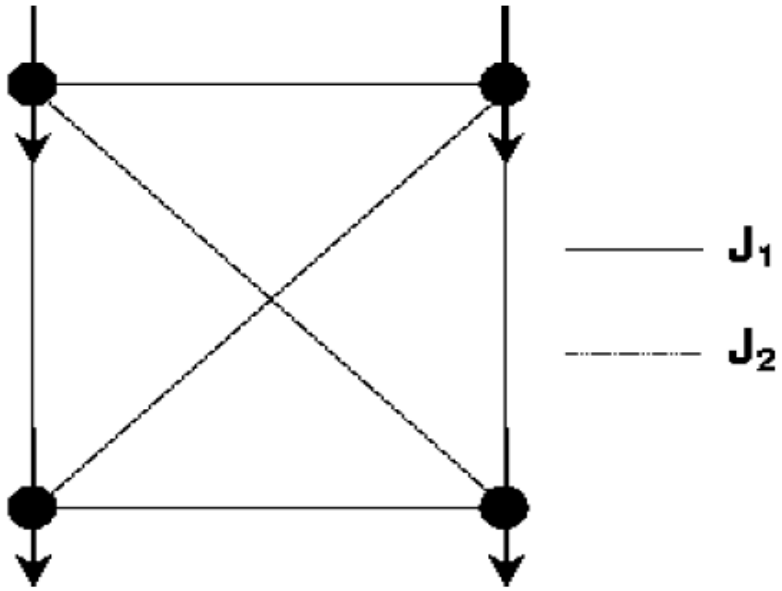

Fig.1.2: Example system frustrated by the geometry of interactions: the square lattice with ferromagnetic interactions between nearest neighbors, and second antiferromagnetic between neighbors [18].

The investigator has little control over the range of interactions, and the vast majority of geometrically frustrated compounds encountered in nature are AF networks based on triangles. To our knowledge, only LiVOSiO4 compounds and LiVOGeO4 spin S = 1/2 Heisenberg may exhibit geometrical frustration induced interactions. In the following, we will focus exclusively on frustration with the network geometry [19].

1.6- Frustration by disorder

Two types of disorder can lead to frustration: the mess in the coupling between the spins, or in the positions of spins. An example of frustration induced disorder couplings is that of the square network: this network nodes are occupied by a spin, so there is no position of confusion, but the interactions that supposed to exist only between nearest neighbors are randomly ± J. according to the criterion of Toulouse [20], a wafer having an even number of ferromagnetic interactions (or antiferromagnetic), is not frustrated: the four couplings can be met simultaneously. If, against the number of links ferromagnetic (or antiferromagnetic) is odd, any of the configurations of the spins can not simultaneously minimize all interaction energies, the wafer is then frustrated.

1.7-The spin glasse

1.7.1-Glasses metal spin

Les verres de spin classiques ou canoniques résultent de la dilution à très faible pourcentage d'impuretés magnétiques (métaux de transition : Mn, Fe) dans une matrice non magnétique (métaux nobles : Ag, Au, Cu, Pt). Le moment magnétique d'une impureté produit une polarisation magnétique des électrons de conduction du métal hôte qui est positive à certaines distances, et négative à d'autres. Les moments magnétiques des autres impuretés sentent le champ magnétique local produit par les électrons de conduction polarisés et tentent de s'aligner avec lui [21,22, 23]. Plus précisément, les interactions entre les spins sont de type oscillant RKKY.

1.7.2-Glasses insulating spin

For a spin-glass, it is not necessary that the interaction is at long range. An example of a system completely frustrated and short-range interaction is given by the antiferromagnetic triangular lattice. An insulator having no conduction electrons, can become a spin glass. Super exchange is a mechanism of interaction between the spins very common in these glasses insulating spin: the antiferromagnetic coupling between two magnetic ions, in a state of E (f), is provided by a ligand or an intermediate anion (in state p) which transfers them an electron through a covalent mixture of the wave functions p and d (or f). But the super exchange may also lead to a ferromagnetic coupling of the spins, bringing again a competition between interactions necessary for the formation of a spin glass. 2.7.3.

1.8-Characteristic properties of spin glasses

This section does not claim to provide a comprehensive list of experimental properties of spin glasses, but only briefly present those that seem most important to the result of this work. The historic kick that started the interest in spin glasses began in 1972 after a magnetic susceptibility of experience in alloy AuFe by V. Cannela and J.A. Mydosh. Their interpretation is based on the existence of a phase transition. Mydosh defined in brief what a spin glass according to some experimental results:

- Measuring the alternative susceptibility.
- The measurement of the specific heat.

- The variation of the magnetization with a magnetic field applied in the low temperature phase.

1.9-Measuring susceptibility

There are several methods for determining the magnetic susceptibility of a material. Static field H small enough, we can measure the magnetization M and divide by the field. Another technique is to apply a weak alternating field h, and measured by taking the derivative dM / dh at a certain frequency w, possibly in a field H bunk.

- **T>>Tg**

  At very high temperatures, it is expected that a spin glass is a simple paramagnetic. The susceptibility measurements in weak field and at very high temperatures indicate that indeed χ follows a Curie-Weiss:

  χ = c/T-θ= NμB2g2J(J+1)/3kB(T-Θ)

- **T <<Tg**

Spin glasses are characterized primarily by the appearance of magnetic irreversibility below a defined temperature Tg. The magnetization measured under static field H depends on whether the sample has been previously cooled under field (FC, field or cooled) or zero field (ZFC, or zero field cooled). A curve representing the magnetization ZFC and FC in the case of CuMn 3% is reproduced on Fig.1.3. The magnetization CF generally has a plateau below Tg and low drift with time. Tg freezing temperature defined as the appearance of irreversibility therefore also depends very slightly time. This behavior is in the alternative susceptibility measurements: one that depends her frequency. It was only in the 70s that the first was discovered the existence of a sharp peak at Tg ac susceptibility in spin glasses, and the presence of this peak was the first evidence of existence of a genuine phase transition. Applying a superimposed static field H has the effect of blunting this peak until making disappear if its big enough st value. the inset of the Fig.1.4 which shows curves of susceptibility as a function of temperature for different frequencies to a sample of CuMn, according Mulder and al.Lors alternative susceptibility measurements a distinction must be drawn between the real part or phase χ '(dispersion) and the imaginary part or out χ' '(uptake) of χ:

$$\chi(w,T) = \chi'(w,t) + i\chi''(w,T)$$

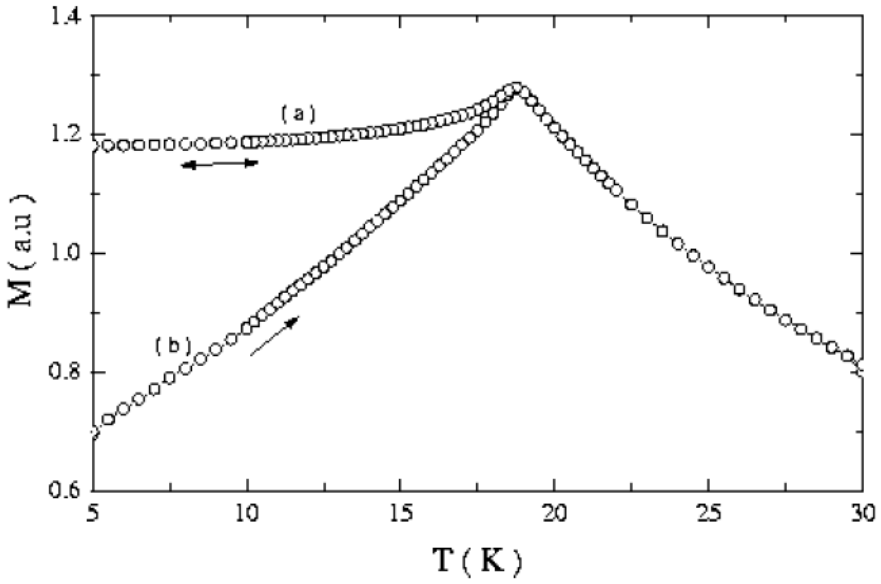

Fig.1.3: Magnetization (a): FC and (b): CFZ depending on the temperature under H = 5G in the case of CuMn 3% [18]

Figure 1.4 shows the temperature dependence of the real and imaginary part of the susceptibility χ alternative a spin glass, according Huser et al. . We observe a sudden appearance of the component out of phase χ " susceptibility Tg near the peak of χ ', so Tg is in fact the most of the slope of χ' 'dχ' '/ dT. The appearance of a component out of phase in susceptibility indicates the presence of relaxation effects.

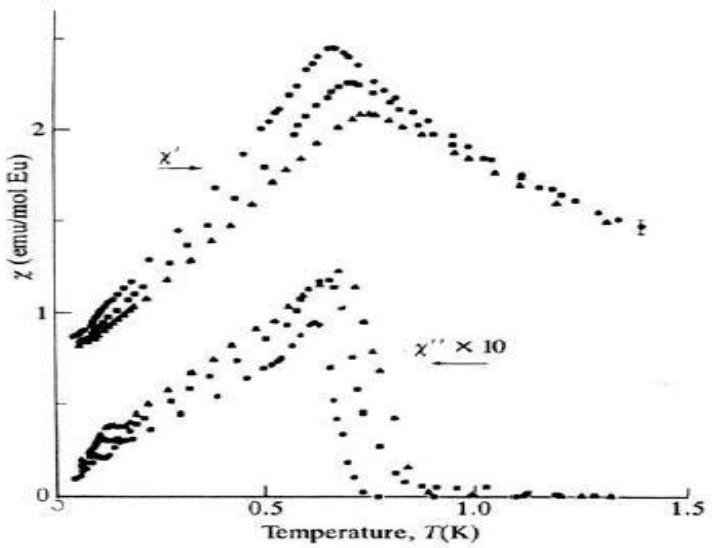

Fig.1.4: the real parts temperature dependence (top) and imaginary (bottom) of the alternative susceptibility of a sample of Eu0.2Sr0.8S [18]

Chapter 02

Fundamentals of Electron Spin Resonance (ESR) Spectroscopy

The following short introduction to the magnetic resonance of exchange coupled spins is confined to the basics necessary to understand the results presented in this thesis. A fundamental introduction to electron spin resonance is given for example by Stephen Blundell [24]. The ESR of diluted transition-metal ions is described in detail by Abragam [24].

2.1. Introduction

Since the first observation by Zavoisky (1945) and the subsequent observation by Cummerow and Halliday (1946), "Electron Spin Resonance" (ESR) technique has initially been applied to non-interacting paramagnetic substances, commonly referred to as "Electron Paramagnetic Resonance" (EPR). There followed an important and fruitful period (1950-1960) of EPR research, in which much of our present-day understanding of paramagnetic ions was established. The technique was immediately applied to ordered ferromagnets by Griffiths (1946) and Kittel (1947), referred to as "Ferromagnetic Resonance" (FMR) and to antiferromagnets by Pauli (1953), referred to as "Antiferromagnetic Resonance" (AFMR). Both FMR and AFMR in the magnetically ordered phases represent a coherent precession of the entire magnetization or sublattice magnetization around the effective fields and are often characterized by a nonlinear dependence of the resonance frequency on the external field, in contrast to the linear behavior usually observed in EPR[25].

It is widely recognized that ESR technique is a very powerful and useful tool to study the magnetic properties from a microscopic point of view. In the past, quite a lot of ESR studies have been devoted to various magnetic compounds, in order to elucidate the magnetic interactions, magnetic ground states, collective motions of interacting spin systems, critical behaviours near the phase transitions, and so on.

2.2. Basic EPR Theory

The phenomenon of electron paramagnetic resonance (EPR) is based on the fact that the electron is a charged particle which effectively "spins" around its axis. In technical language we say : the electron has a magnetic moment $\vec{\mu}$ due to its spin $\vec{S}$:

$$\vec{\mu} = -g\mu_B\vec{S} = -\gamma_e\hbar\vec{S} \qquad (2.1)$$

where the proportionality is expressed in terms of the Bohr-magneton $\mu_B = \frac{e\hbar}{2m_e}$ or gyromagnetic ratio $\gamma_e = \frac{g\mu_B}{\hbar}$.

Here g is the electronic g-value, for the free electron $g_e = 2.002319$, $\hbar = h/2\pi$ with Planck constant h, e is the elementary charge and m_e the electron mass.

For a spin ½ system, in the absence of an external magnetic field, the two possible spin states with spin quantum numbers $m_s = +1/2$ and $m_s = -1/2$ have the same energy and are equally populated. If an external magnetic field $\vec{H}_0 = H_0\hat{z}$ is applied to the system, the degeneracy of the spin states will be lifted (the so-called Zeeman splitting Figure 1.1). The Zeeman operator reads $H_{Zeeman} = -\vec{\mu}\cdot\vec{H} = g\mu_B S_z H_z$ with the eigen energies $E = \pm\frac{1}{2}g\mu_B H_z$ for spin up and down, respectively. This means that the magnetic field will divide the electrons into two groups. In one group the magnetic moments of the electrons are aligned parallel to the magnetic field, while in the other group the magnetic moments are aligned antiparallel to the external field. The energy difference between the two states becomes $\Delta E = g\mu_B H_0$. If a second weaker alternating magnetic field $\vec{H}_1$ oscillating at a microwave frequency ν is now applied perpendicular to the static field $\vec{H}_0$ (as shown in Figure 2.2), then the electron spin can be tipped over, if the microwave frequency is equal to the energy-difference ΔE between the Zeeman levels:

$$\Delta E = h\nu = g\mu_B H_{res} \qquad (2.2)$$

The incoming radiation $h\nu$ absorbed by the electrons in the lower energy level will induce them to jump into the higher energy state. However, the electrons in the higher energy level jump down to the lower level, a phenomenon called stimulated emission. Since the

coefficients of absorption and stimulated emission are equal, no net value would be observed, if the spin population were equally distributed between these two levels. In general, in the thermal equilibrium the population of the ground state n_1 exceeds the population of the excited state n_2, and a net absorption of microwave radiation takes place. The polarization of the system is brought back towards a Boltzmann probability expression:

$$n_1/n_2 = \exp(-\Delta E/k_B T) \qquad (2.3)$$

where k_B is the Boltzmann constant. Thus the system can absorb the electromagnetic radiation from an external source of frequency ν, if the basic resonance condition is fulfilled. Since ESR measures absorption, due to the slightly greater population of the lower level, this difference should be made as large as possible to enhance the measured signal. For that, one can measure at low temperatures or use a high magnetic field. The ratio n_1/n_2 is approximately 0.999 if one uses an X-band spectrometer ($\nu = 9.5\,\mathrm{GHz}$) at room temperature, this means even with a very small difference in the population one can see the ESR signal for a lot of materials [25].

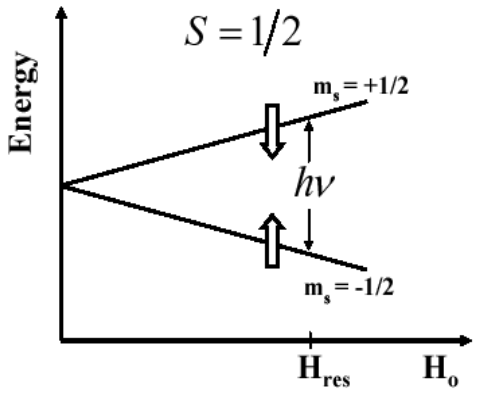

Fig. 2.1: Zeeman splitting of the free electron spin levels in an external magnetic field [25].

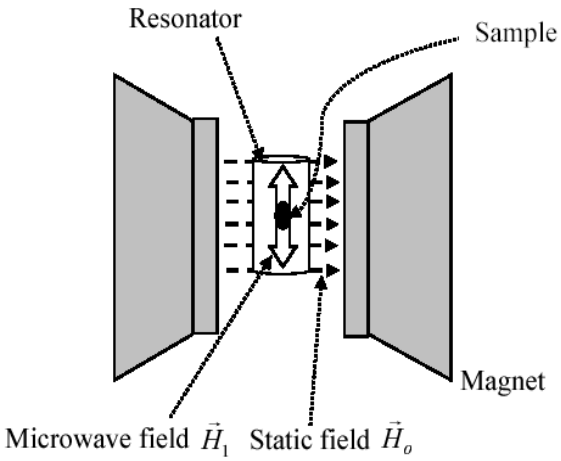

Fig. 2.2: Principle arrangement of the ESR experiment showing the direction of the microwave magnetic field ($\vec{H}_1$) with respect to the static magnetic field ($\vec{H}_0$) [25]

After absorption of energy the polarization may change, but if the electron spin system interacts with the thermal motion and excitations of the sample, the polarization of the spin system can return towards its equilibrium value. If the polarization of the spin system has been reduced to zero by rapid electromagnetic transitions, the spin system will take some time to "recover" once the electromagnetic irradiation is switched off; this time is called T_1 and measures the time constant of the interaction between the spin system and its surroundings. T_1 is the spin-lattice relaxation time (sometimes called the longitudinal relaxation time). If we take an equilibrium value of magnetization M_0 with the static magnetic field B_0 applied along the z-axis, the microwave frequency excitations will progressively destroy this magnetization. After switching of the microwave, we expect that

$$\frac{dM_z}{dt} = \frac{M_0 - M_z}{T_1} \qquad (2.4)$$

The relaxation T_1 must involve interactions with the lattice, because changing M_z has energetic consequences, since relaxing a spin in the z-direction changes its orientation with respect to the applied field, and hence changes its energy. The M_x and M_y components should be zero in thermal equilibrium. After microwave irradiation they will relax back to zero in a time T_2 such that

$$\frac{dM_x}{dt} = -\frac{M_x}{T_2}, \qquad \frac{dM_y}{dt} = -\frac{M_y}{T_2} \tag{2.5}$$

T_2 is the spin-spin relaxation time (the transversal relaxation time) and is the characteristic time for dephasing of the spins, because it corresponds to the interaction between different parts of the spin system. It can also be due to inhomogeneities in the magnetic field B_0. It thus leads to differences in precession frequency due to the interactions between the observed spin and the spins of its neighbours. Changing M_x or M_y has no energetic consequences because the applied field is along M_z.

The equation of motion of the magnetization is derived from the torque due to the applied field B_0. Using equation (1.1) and summing over all spins the time derivative of the spin is translated into the time derivative of the magnetization. The equation of motion reads: $\vec{M} = -\gamma \vec{M} \times \vec{H}$, which describes the precession of $\vec{M}$ around $\vec{H}$ with Larmor frequency $\omega_L = \gamma H$.

Including the relaxation terms (1.4) and (1.5), discussed above, we obtain

$$\frac{d\vec{M}_z}{dt} = -\left(\vec{M} \times \gamma_e \vec{H}\right)_z + \frac{\vec{M}_0 - \vec{M}_z}{T_1} \tag{2.6}$$

$$\frac{d\vec{M}_i}{dt} = -\left(\vec{M} \times \gamma_e \vec{H}\right)_i - \frac{\vec{M}_i}{T_2} \tag{2.7}$$

where i denotes x or y. These equations are known as the Bloch equations. They can be solved for a number of cases of interest, very often by using a rotating reference frame method in which the coordinates are changed to ones which rotate in the xy-plane at the resonance frequency.

2.3. ESR Parameters

It is important to show which quantities are accessible during an ESR experiment and how the desired microscopic information can be deduced from these quantities. A lot of information can be deduced from the electron spin resonance absorption spectra. The main four characteristics which can be deduced are the lineshape and the linewidth, the g-factor and the spin susceptibility.

2.3.1. Linewidth and lineshape

A great deal of information about the studied spin system can be obtained from a careful analysis of the width and the shape of the resonant absorption line. The experimentally observed ESR lineshapes in a large variety of materials can often be fitted by a Dysonian (modified Lorentzian) lineshape, regardless if they are being metallic or regardless of insulating and the dimensionality of the spin system.

$$P_{abs}(H) \propto \frac{\Delta H + \alpha(H - H_{res})}{(H - H_{res})^2 + \Delta H^2} \qquad (2.8)$$

where $0 \le \alpha \le 1$. By solving Bloch equations (1.7) which are describe the transversal components of magnetization, by substituting $M^+ = M_x + i M_y$ and $M^+ = \chi(\omega) H_1 e^{i\omega t}$ (where $e^{i\omega t}$ is a circular polarization), the dynamic susceptibility $\chi(\omega) = \chi'(\omega) - i\chi''(\omega)$ and, therefore, the shape of the absorption ESR line can be deduced. Far from the saturation, the microwave absorption power corresponds to a pure Lorentz line equation (1.8) with $\alpha = 0$. The admixture of dispersion ($\alpha \neq 0$) in real spectra can result from non zero conductivity or in the case of broad resonance lines in low crystallographic symmetry.

Note that in ESR one mostly encounters the so-called peak-to-peak linewidth (ΔH_{pp}) which is defined as the distance between points of maximum slope of the absorption line (see Figure 1.4). In the first derivative this appears simply as the distance between the maximum and the minimum of the curve, this explains its wide-spread use in ESR practice. The peak-to-peak linewidth differs from the half width at half maximum (HWHM or ΔH) by a numerical factor which depends on the particular lineshape (for a Lorentzian line $\Delta H = \sqrt{3}\Delta H_{pp}/2$).

In the present work strongly exchange-coupled spin systems are considered, where the spectra are fully exchange narrowed Lorentz lines. In the high-temperature approximation the corresponding linewidth is given by the relation:

$$\Delta H \approx \frac{\hbar^2}{g\mu_B |J|} M_2 \qquad (2.9)$$

where M_2 is the second moment of the resonance field distribution due to antiferromagnetic spin-spin interaction and J is the isotropic exchange coupling constant.

2.3.2. Resonance Field and g-Factor

Recalling the resonance condition (see equation 1.2), one has to take into account that local magnetic fields H_{loc} will be present at the spin's site in addition to the external magnetic field H_{ext}. Hence, the fit parameter $H_{res} = H_{ext} + H_{loc}$ or the resulting effective g-factor of the free electron $g_e = 2.0023$

$$g_{eff} = \frac{\hbar\omega}{\mu_B H_{res}} \qquad \Delta g = g_{eff} - g_e \tag{2.10}$$

provide a measure for local fields at the spin's site.

2.4. Spin susceptibility

For any system under magnetic resonance, one has to consider the complex magnetic susceptibility

$$\chi(\omega) = \chi'(\omega) - i\chi''(\omega) \tag{2.11}$$

where the real part produces a frequency change in the resonance cavity and the imaginary part leads to energy absorption. The microwave absorbed power P_{abs} is proportional to $\chi''(\omega)$. From Kramers-Kronig relations we get for the electron spin susceptibility χ_e^s:

$$\chi_e^s = \frac{2}{\pi H_{res}} \int_0^\infty \chi''(H)dH \propto \int_0^\infty P_{abs}(H)dH = I \tag{2.12}$$

The intensity I of a Lorentzian absorption line is given by

$$I = \frac{2\pi}{\sqrt{3}} y'_{max} \Delta H_{pp}^2 \tag{2.13}$$

where ΔH_{pp} is the peak to peak linewidth and y'_{max} is the maximum amplitude of the derivative of the ESR absorption signal. Since χ_e^s is proportional to I, only a relative value of the spin susceptibility can be measured by ESR.

The absolute value of the spin susceptibility can be determined by comparing the intensity of the ESR signal with the intensity of the ESR line of a standard sample of known spin susceptibility as for example a DPPH sample.

2.5. ESR Apparatus

For the ESR measurements in this work a commercial continuous wave (CW) X-band spectrometer (BRUKER Elexsys 500) was used. The microwave source is a Gunn diode operating at a frequency 9.5 GHz and a maximum power output 200 mW. Figure 1.3 shows the general layout of the ESR spectrometer.

The electromagnetic radiation source and the Schottky barrier detector diode are in a box called the microwave bridge. The sample is in a microwave resonator (cavity), (see section 1.4.1). The field strength of the electromagnet, which ranges from -50 to 18000 G, is measured and controlled by the field controller. The computer is used for coordinating the units for acquiring a spectrum. Although many spectrometer designs have been produced over the previous years, the vast majority of laboratory instruments are based on the simplified block diagram shown in Figure 2.3.

The output power of the Gunn diode can be varied using the attenuator, a device which blocks the flow of the microwave radiation. With the attenuator, one can precisely and accurately control the output microwave power.

The BRUKER Elexsys 500 is a reflection spectrometer; this means it measures the changes (due to spectroscopic transitions) in the amount of radiation reflected back from the microwave cavity. The direction of the microwave radiation is controlled by the circulator, where the microwaves coming from the klystron through the circulator only go to the cavity and not directly to the detector, and the reflected microwaves are directed only to the detector and not back to the microwave source. The detector diode is mounted along the E-vector of the plane-polarized microwaves and thus produces a DC proportional to the microwave power reflected from the cavity. Thus, in principle, the absorption of microwaves by the sample can be detected by noting a decrease in the DC which can be measured by a micrometer. In practice such a DC would be far too noisy to be useful. To increase the signal-to-noise ratio, small amplitude field modulation is introduced. An oscillating magnetic field is super-imposed on the DC field by means of small modulation coils, usually built into the cavity walls.

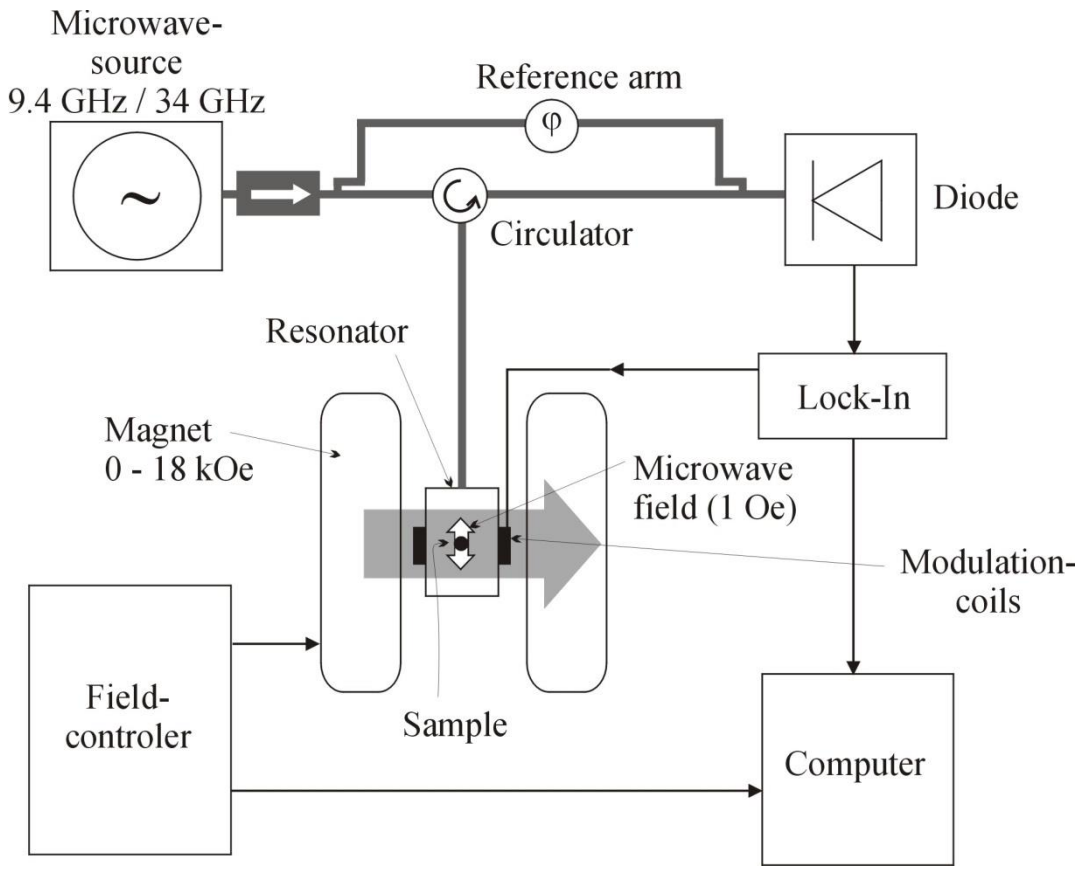

Fig. 2.3: Block diagram of the ESR (BRUKER ESP 300) spectrometer [25].

When the field is in the vicinity of the resonance line, the modulation field is swept back and forth through part of the line, leading to an AC component in the diode current. This AC component is amplified using a frequency selective amplifier with small bandwidth (lock in amplifier), thus eliminating a great deal of noise. The modulation amplitude is normally less than one tenth of the linewidth. Therefore the detected AC signal is proportional to the change in sample absorption. As a result of modulating the magnetic field, the detected signal appears as the first derivative of the absorption signal, as shown in Figure 2.4. In all ESR measurements of this work the modulation frequency was 100 KHz.

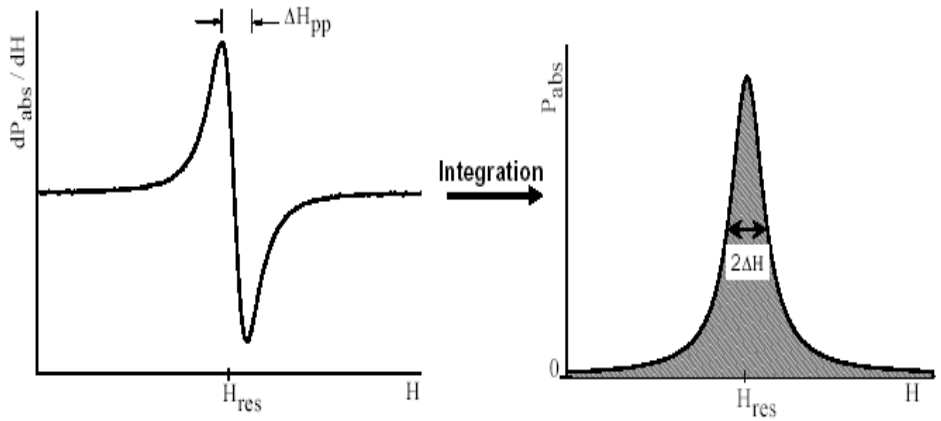

Fig. 2.4: The derivative of the ESR absorption signal dP_{abs}/dH ***(which is measured directly by the ESR apparatus)(left), and the absorption signal*** P_{abs} ***(right) as a function of the static magnetic field. The area under the absorption line is proportional to the spin susceptibility [25].***

The microwave cavity is a box fabricated normally from highly conductive metal with dimensions comparable to the wavelength. At resonance, such a cavity sustains microwave oscillations, which form an interference pattern (standing wave configuration) from superposed microwaves multiply reflected from the cavity walls. This means that the cavity stores the microwave energy; therefore, at the resonance frequency no microwaves will be reflected back from the cavity, but will remain inside it. Each particular cavity size and shape can sustain oscillations in a number of different standing wave configurations called modes.
Cavities are characterized by their quality factor (Q), which indicates how efficiently the cavity stores microwave energy. As the quality factor increases, the sensitivity of the spectrometer increases. The quality factor of a cavity is defined as:

$$Q = \frac{2\pi(\text{power stored in the cavity})}{(\text{power dissipated per cycle})} \qquad (2.14)$$

Energy can be dissipated to the side walls of the cavity because the microwaves generate electric current in the side walls which in turn generates heat, therefore the quality factor of the cavity depends on the conductivity of the material from which the cavity is made and the geometry of the cavity. ESR measures magnetic dipolar transitions between the Zeeman

levels. Thus, it is the magnetic component of the microwave field that drives the absorption in ESR. Therefore the sample has to be placed in the electric field minimum and the magnetic field maximum to obtain the largest signal and the highest sensitivity of the cavity.

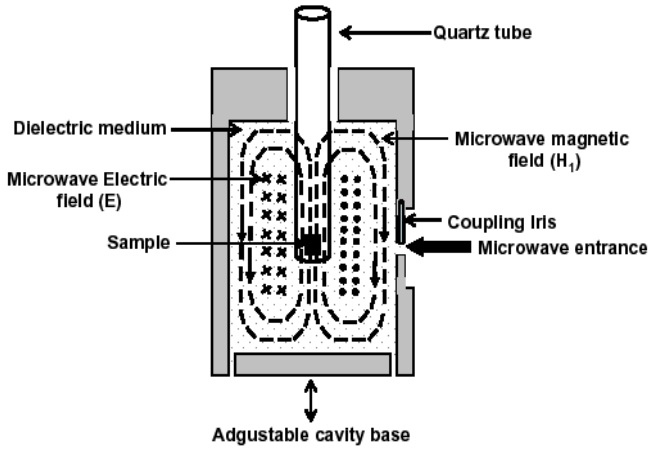

Fig. 2.5: ESR cavity[25]

Chapter 03

Results and discussions

The resulting magnetic properties of CuCrSnS4 have received a renewed attention from theoretical as well as experimental point of view, because these materials can exhibit spin-glass behaviour [17] and show a magneto-optical Kerr effect. Below a certain freezing temperature T_f, the spin-glass state arises from disorder due to dilution and underlying frustration of the magnetic interactions between the localized magnetic moments. The frustration may be due to competing ferromagnetic (F) and antiferromagnetic (AF) exchange interactions or result from purely topological effects, when the interactions are predominantly AF. In the pseudo-binary systems $CuCrS_2$-MS_2 (M = Ti, Sn), spinel phases of the composition $Cu_{2x}Cr_{2x}M_{2-2x}S_4$ have been discovered [18,19]. Their homogeneity range is wide: $0.68 \leq 2x \leq 1.26$ for M = Ti and $0.2 \leq 2x \leq 1.36$ for M = Sn. For $2x = 1$, the Cu^{1+} ions fully occupy the tetrahedral A sites, whereas the paramagnetic Cr^{3+} ions and the diamagnetic M^{4+} ions remain located on the B sites. X-ray diffraction did not show any ordering to occur between Cr^{3+} and M^{4+} ions.

The experimental evidence, to date, indicates that the $Cu_{2x}Cr_{2x}M_{2-2x}S_4$ spinels are spin-glasses. These systems are very sensitive to the methods of preparation and deviations from stoichiometry [20]. This effect was discussed with respect to a deficiency and excess of cations in tetrahedral or octahedral voids of the spinel structure. In this series, when the stoichiometric composition is passed through as $2x$ increases, drastic changes occur in (i) the electric resistivity: the activation energy drops [18,19], (ii) magnetic susceptibility: the Curie-Weiss temperature θ_p changes from negative to positive values, which indicates that additional ferromagnetic couplings appear [18,19], and (iii) electron spin resonance (ESR): the line width passes through a maximum close to $x \sim 0.5$ and rapidly decreases for larger x, which suggests an enhancement of the exchange narrowing in the dense magnetic lattice [21]. Although there are numerous data available for powder materials, the studies of the effect of nonmagnetic Zr^{4+} substituted for Cr^{3+} atoms on the properties of the spinel structure are inconsistent. This raises the question about the proper location of the Zr ions and the metal excess of Cu in the spinel structure [22]. Recently the system $Cu(Cr_{1-x}Zr_x)_2S_4$ has been studied [23, 24], where the Cu stoichiometry is kept unchanged. The substitution of Zr for Cr atoms

has introduced antiferromagnetic interactions and spin frustration to the *B* sites resulting in a spin-glass state below $T_g \approx 10$ K. Above T_g the system exhibits a spin-liquid behaviour over a temperature range of $T_g \leq T \leq \theta_p$ limited by the Curie-Weiss temperature, which ranges from $\theta_p = 219$ K for $x = 0.4$ to $\theta_p = 24$ K for $x = 0.55$. In the present work we focus on the corresponding selenide compound $CuCrZrSe_4$ to study the influence of the larger Se anions on tthe magnetic properties.

3. Experimental

Polycrystalline $CuCrZrSe_4$ has been prepared by solid-state reaction from the stoichiometric mixture of the pure elements as described previously [25, 26]. Room-temperature powder x-ray diffraction (XRD) measurements were carried out with a STOE STAD-IP diffractometer (fig.3.1) in the Bragg-Brentano geometry using CuKα radiation (λ = 1.54059 Å). The XRD patterns were recorded from angles 2θ = 10° to 130° with a 0.02° step size. Further analysis was carried out by the Rietveld method using the FULLPROF program [27]. The magnetic properties of the powder sample were studied in the temperature interval from 2 to 400 K using a commercial superconducting quantum interference device (SQUID) magnetometer "MPMS 5" from Quantum Design (fig.3.2). Electron spin resonance (ESR) experiments were performed in a Bruker ELEXSYS E500-CW spectrometer at X-band frequency (f = 9.36 GHz), equipped with a continuous He-gas flow cryostat (Oxford Instruments) working in the temperature range from liquid helium to room temperature (fig.3.3).

Fig.3.1: STOE STAD-IP diffractometer , Experimental Physics V, Centre for Electronic Correlations and Magnetism, Institute of Physics, University of Augsburg, 86135 Augsburg, Germany.

Fig.3.2: superconducting quantum interference device (SQUID) magnetometer "MPMS 5" from Quantum Design Experimental Physics V, Centre for Electronic Correlations and Magnetism, Institute of Physics, University of Augsburg, 86135 Augsburg, Germany.

Fig.3.3.: ESR-Spektrometer Bruker ELEXSYS E500-CW

Experimental Physics V, Centre for Electronic Correlations and Magnetism, Institute of Physics, University of Augsburg, 86135 Augsburg, Germany.

3.1. Results and Discussion

3.1.1. Powder x-ray diffraction

Powder x-ray diffraction studies prove the proper normal spinel phase, which could be indexed satisfactorily based on a cubic cell (space group $Fd\bar{3}m$) with the lattice parameter a = 10.649(2) Å in agreement with Ref. [26]. Fig.3.4 shows the XRD patterns of $CuCrZrSe_4$. The Rietveld refinement was started by using the structural model of $MnSc_2S_4$ and the lattice parameter obtained with the program DICVOL04 [27] . The origin of the unit cell was taken at the point $\bar{3}m$ of the space group $Fd\bar{3}m$ (No. 227 in the International Tables for X-ray Crystallography) with Se in 32e, the tetrahedral site in 8a and the octahedral site in 16d. The refinement of 14 parameters (zero shift, scale factor, asymmetry parameter, and mixing parameter of the pseudo-Voigt peak shape function, unit-cell parameter, positional parameters, and isotropic temperature factor) converged to the final profile yielding agreement factors of R_B = 0.116, R_p = 0.339, and R_{wp} = 0.232. These factor values are fairly large indicating probably a strong local variation of the Cr:Zr ratio. Nevertheless, the difference spectrum shows a good agreement between observed and calculated spectrum.

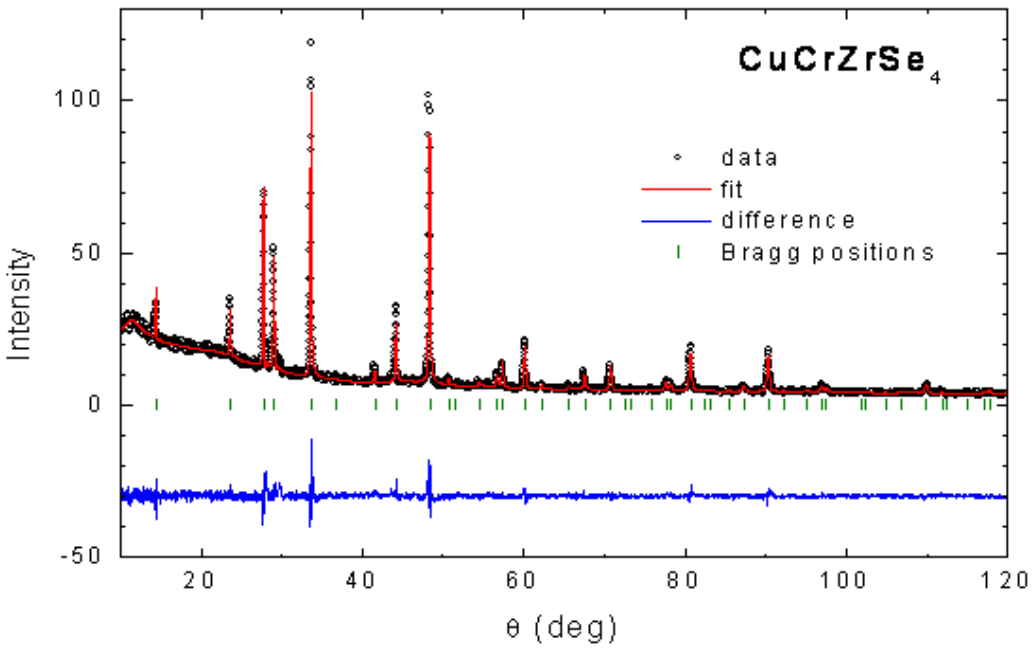

Fig.3.4: Observed and fitted x-ray diffraction profiles of $CuCrZrSe_4$

3.1.3. Magnetic properties

Figure 3.5 shows the temperature dependence of the magnetic susceptibility $x = M/H$ of CuCrZrSe4 derived from the magnetization M measured in an external magnetic field H = 10 kOe. As one can see from the inverse plot 1=_ *vs*: T, the susceptibility follows a Curie-Weiss law for temperatures $T > 250$ K. One obtains a positive Curie-Weiss temperature θp = 115 K and an effective magnetic moment $\mu e f f = 3{:}75 \mu B$ per *Cr* ion. This value is quite close to that calculated for a $Cr3+$ ion with $3d3$ electron configuration in octahedral ligand field (i.e. spin-only half-filled $t2g$ state with spin $S = 3{=}2$ and g value $g = 2$: $\mu e\, f\, f = 3{:}75 \mu B$) and yields g = 1:94 as typical for $3d$ ions with less than half filled $3d$ shell. Taking into account that the undiluted parent compound $CuCr2S\, e4$ undergoes ferromagnetic order already below a Curie temperature of 420 K [28], the large positive value of θp resembles the still dominantly ferromagnetic character of the exchange interactions in the present case of 50% *Zr* substitution on the *B* site.

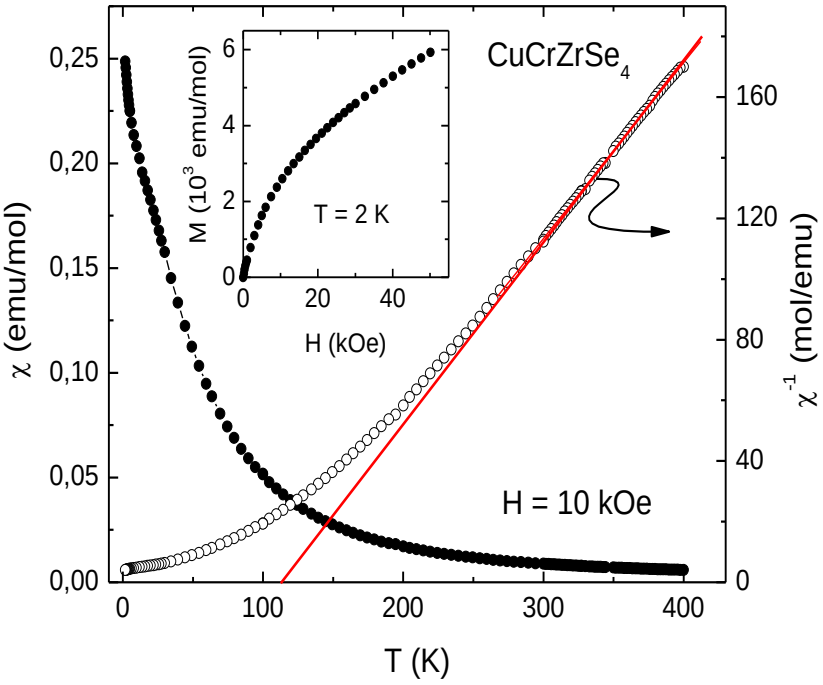

Fig.3.5: Temperature dependence of the susceptibility of $CuCrZrSe_4$ in a DC magnetic field H = 10000 Oe, and the inverse magnetic susceptibility.The straight line indicates the Curie-Weiss law. The inset shows the field dependence of magnetization measured at T = 2K

At lower temperatures, the susceptibility deviates from the Curie-Weiss law and increases monotonously down to the lowest temperature under investigation with a weak anomaly around 10 K. However, the magnetization shown in the inset of Fig. 3.6 does not reach saturation up to fields of 50 kOe at T = 2 K, which indicates that the dilution inhibits a purely ferromagnetic ground state. To give a more detailed characterization of the ground-state properties, Figure 3.6 depicts zero-field cooled (ZFC) and field-cooled (FC) susceptibility measured in an applied field H = 50 G. For the ZFC measurement the compound is cooled from 300 down to 2 K at zero magnetic field, and the field is turned on just before the measurement starts, whereas in the FC measurement the field is switched on, when the compound is paramagnetic before being cooled. With decreasing temperature, ZFC- and FC-susceptibility start to diverge from each other below 100 K with a tendency for saturation below 50 K, but exhibit a second strong divergence below 20 K. In general the saturation-behaviour of the low-field susceptibility indicates the existence of ferromagnetic short range order below 100 K.

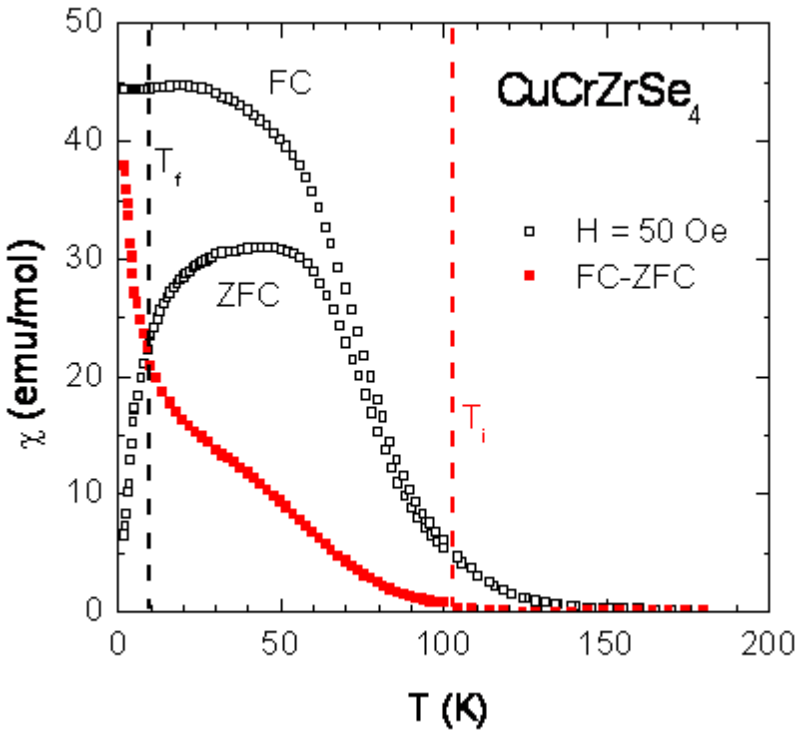

Fig.3.6: Temperature dependence of zero-field cooled (ZFC) and field cooled (FC) susceptibility of CuCrZrSe$_4$ measured in a low DC magnetic field H = 50Oe (open symbols). The closed symbols indicate the difference between FC and ZFC data. Below T_I irreversibility shows up, T_f marks the low-temperature anomaly.

To check whether the observed irreversibility results from the formation of a spin-glass state, we measured the AC susceptibility x*ac*, at an AC field amplitude Hrms = 4 Oe in the frequency range 1−1000 Hz. In the case of a spin glass, both components, real part x′ and imaginary part x″ of x*ac*, should present a sharp, frequency dependent anomaly. The position of the cusp in x′ defines the freezing temperature *T f*, which is coincident with the temperature of the inflexion point in x″ (Fig. 3.7)

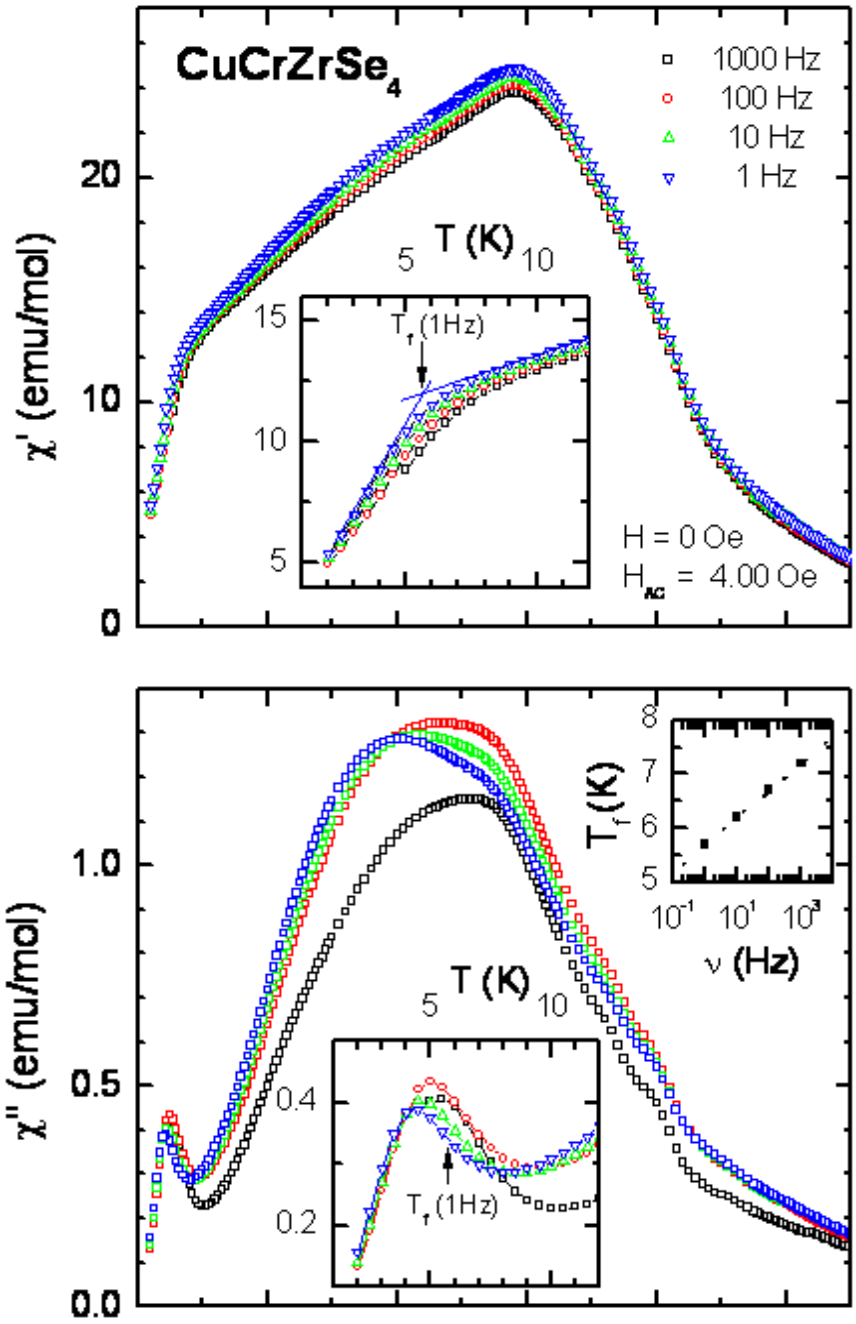

Fig.3.7: The temperature dependence of real (upper frame) and imaginary part (lower frame) of the AC susceptibility of $CuCrZrSe_4$ at different frequencies

As shown in fig.3.7 x' exhibits a broad maximum centered at 58 K and a shoulder close to 7*K*. While the maximum does not change its position with increasing frequency, the low-temperature shoulder clearly shifts to higher temperatures as the frequency of the AC field is increased. In the same low-temperature regime one observes a comparably frequency-dependent inflexion point in x″. But for higher temperature the imaginary part is dominated by a broad maximum, which shifts from about 40 K at 1 Hz up to 51 K at 1000 Hz with no clear correspondence in the real part. A closer inspection, shown in the upper inset of the lower frame in Fig. 3.7, yields a linear relation between the logarithm of the applied frequency and the temperature of the low-temperature shoulder in x′ as well as of the corresponding inflexion point in x″, as expected for the freezing temperature of a spin glass. Thus, a spin-glass state is evidently realized below $T f \approx 5 - 7$ K. However the irreversibility at higher temperature is probably not of intrinsic origin but related to the pinning of magnetic domain walls at the grain boundaries of the polycrystalline sample [31]. To explain the appearance of the spin-glass states in the sample under study one has to take into account the electronic configuration of the CuCr2Se4 matrix. In that compound the mixed valence $Cr3+ - Cr4+$ is responsible for the double exchange magnetic interaction, which gives a dominantly ferromagnetic coupling. On the other hand there exist simultaneously super-exchange interactions, which in turn give both ferro (nearest-neighbour 90◦ exchange) and antiferromagnetic (next-nearest neighbour) couplings [32]. Substituting 50% nonmagnetic zirconium ions ($Zr4+$) instead of the magnetic chromium ions ($Cr4+$) completely suppresses the ferromagnetic double exchange and partially inhibits the nearest neighbour ferromagnetic super exchange. At the same time the antiferromagnetic components of the super exchange are promoted. The statistical character of this effect leads to the frustration of the orientations of the localized magnetic moments in the sample under study and in the consequence to the appearance of the spin-glass state [29,30].

3.3. ESR studies

A microscopic access to the magnetic properties is provided via ESR which detects the microwave absorption du to magnetic dipolar transitions between the Zeeman levels of the magnetic ions. The ESR spectra are taken at constant microwave frequency f = 9:36 GHz dependent on the external static magnetic field H. Due to the lock-in technique 3

with field modulation the field derivative of the absorption signal is recorded. Fig.3.8 shows typical examples of spectra obtained in *CuCrZrS e*4 at different temperatures. The signals are well described by two Lorentz curves of different line width at approximately the same resonance field corresponding to a g value $g = h f =\_B H_{res} \approx 0{:}2$, typical for Cr^{3+} where the orbital momentum is nearly quenched by the ligand field [31,32,33].

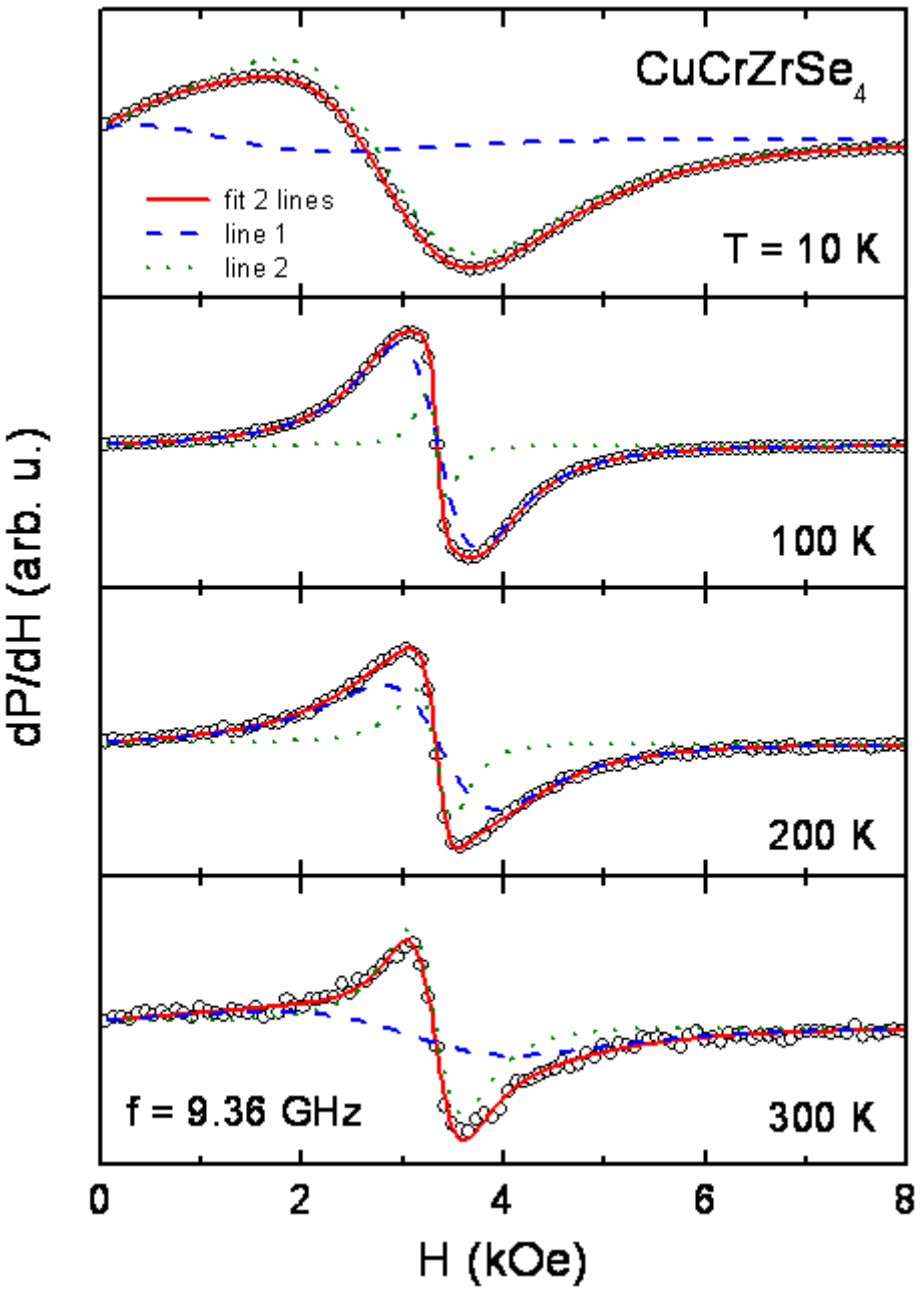

Fig.3.8: Temperature evolution of the ESR spectra of $CuCrZrSe_4$. The solid line indicates the fit with a sum of two Lorentz curves (dashed and dotted lines).

The temperature dependence of the fit parameters – intensity, resonance field, and line width (half width at half maximum) – is depicted in Fig.3.9

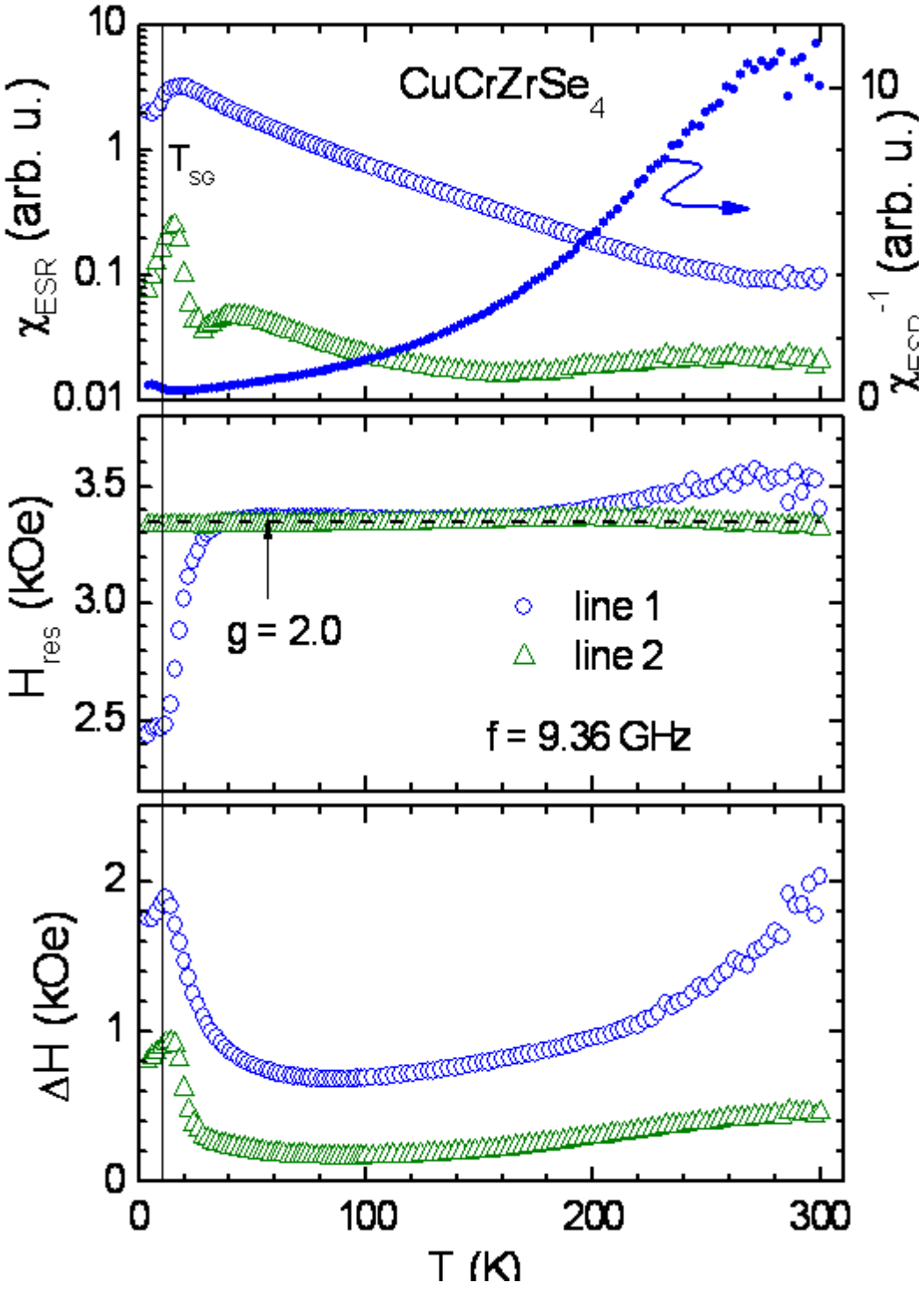

Fig.3.9: Temperature dependence of spin susceptibility χ_{ESR} (upper frame) and the inverse 1/ χ_{ESR} of the main component, resonance field H_{res} (middle frame), and linewidth ΔH (lower frame) in $CuCrZrSe_4$

The broad line with a width of the order of 1 kOe yields the main contribution to the ESR absorption: its intensity x*ES R* increases monotonously with decreasing temperature up to the maximum at about 20 K. Below the line shifts away from $g = 2$ to lower resonance fields accompanied by a slight decrease of the intensity. In inverse representation 1/x*ES R* nicely compares with the inverse static susceptibility, following a Curie-Weiss law above 180 K and revealing a positive curvature at lower temperatures. The corresponding line width exhibits a maximum at about 15 K, decreases with increasing temperature up to 90 K and then increases again above 90 K. The width of the second line is about 5 times smaller than that of the main line and also increases on increasing temperature, while the corresponding intensity is approximately constant. However the pronounced peak in the intensity of the second line and the sudden increase of its line width below 20 K is presumably an artefact connected with the shift and distortion of the first line at 20 K, because here the fit procedure cannot accurately separate both lines anymore. The approximately constant intensity of the weak line indicates that it originates from a ferromagnetic contribution of a small amount of foreign phase, probably CuCr2Se4 [34]. From the intensity ratio of narrow to broad line, which is smaller than 20 at lowest temperature, we can estimate that the amount of foreign phase is at least less than 5 atomic percent, which is below the resolution limit of *x*-ray diffraction. Probably the amount is even smaller, if we assume that the spins of the ferromagnetic foreign phase are fully aligned, which is not the case on the spin-glass state of the main phase. The strong line can be ascribed to the *Cr*3+ ions in the proper phase. The line width can be understood to originate from the competition between broadening sources (hyperfine coupling, dipole spin-spin interactions, and singlephonon spin-lattice relaxation) and narrowing process (exchange-narrowed relaxation) [35, 36].

Note that the temperature dependence and absolute value of the line width is rather similar to the one observed in Cu2xCr2xS n2−2xS 4 [21]. In that reference the dipolar interaction between the Cr ions was identified as the main source of line broadening under the condition of a strongly inhibited exchange narrowing. In case of usual exchange narrowing a line width smaller by two orders of magnitude is expected from the Weiss constant derived from magnetic susceptibility in CuCrZrSe4. However in the case of dominantly antiferromagnetically frustrated spin glasses the dipolar interactions between uncompensated spins on different spin clusters are not averaged out by the exchange interaction, resulting in

the large observed line width [21]. Note that two sources of broadening, which are often discussed as leading contributions in transition-metal compounds, i.e. the crystal-electric field and the Dzyaloshiskii-Moriya antisymmetric exchange interaction [37, 38, 39], can be neglected in the present case due to the following reasons: (i) From our Rietveld refinement we can exclude any structural deformations of the octahedral and tetrahedral sites. Thus, the Cr3+ ions are found in a purely cubic crystal field on the octahedral sites. In a cubic crystal field the degeneracy of a $S = 3=2$ spin quadruplet is not lifted and, therefore, the Zeeman splitting in an external field remains equidistant. So there is no splitting of the magnetic dipolar transitions and in turn the broadening contribution of the crystal field vanishes. (ii) The Dzyaloshinskii-Moriya interaction can be excluded as well due to the high symmetry of the ideal spinel structure where the antisymmetric exchange contributions fully cancel each other.

General conclusion

In conclusion, polycrystalline CuCrZrSe4 has been studied by x-ray powder diffraction, magnetic susceptibility, and ESR measurements. It belongs to the normal spinel structural type, the Cu1+ ions are exclusively located on the tetrahedral position 8*a* : (1=8; 1=8; 1=8), while Zr4+ and the Cr3+ ions share the octahedral position 16*d* : (1=2; 1=2; 1=2). No sign of any ordering of the *Cr* and *Zr* ions is observed. The magnetic properties are comparable to those of the related sulphide spinels.

The substitution of nonmagnetic *Zr* for *Cr* atoms weakens the ferromagnetic nearest-neighbour exchange between the *Cr* ions in favour of the remaining antiferromagnetic next-nearest neighbor interactions and resulting geometrical spin frustration of the *B* sites. The positive Curie-Weiss temperature θp = 115 K and the onset of irreversibility below $TI \approx$ 100 K indicate ferromagnetic short-range order in the temperature range of $T f \leq T \leq \theta p$, while long-range magnetic order cannot develop due to frustration and disorder. Only below $T f \approx$ 7 K, the spin system freezes into a spin-glass state.

Regarding the related sulfid spinels indicates that the size of the *X*-ion is of minor importance compared to the effect of dilution of the Cr ions by non magnetic Zr ions,4 which gives rise to disorder and competing antiferromagnetic interactions between the Cr spins. Both the Curie-Weiss temperature and the temperature of the spin-glass transition exhibit values which are comparable to each other in the Se and the S compounds.

References

[1] C.A. Jouenne –Traité de Céramiques Et Matériaux Minéraux–Ed. Septima, Paris (1990).

[2] S.M. Yunus, H.-S. Shim, C.-H. Lee, M.A. Asgar, F.U. Ahmed & A.K.M. Zakaria, J. M. M. M 40–50 (2002)

[3] J. Dorman et al, J. Phys. Condens. Matter. 2, 1223 (1990).

[4] D. Fiorani et al. Phys. Rev. B 30, 1776 (1984).

[5] J. K. Srivastava et al. Phys. Lett. A 121, 322 (1987).

[6] P. Barahonaa & O. Penaa, Physica B 384, 74–77(2006)

[7] G.M. Kalvius, O. Hartmann, D.R. Noakes, F.E. Wagner, R. Wappling, U. Zimmermann, Ch. Baines, A. Krimmel, V. Tsurkan & A. Loidl, Physica B 592–593–(2006)

[8] V. Eyert, K.H. Hock, S. Horn, A. Loid & P. S. Riseborough, Euro. Phys. Lett.46 762-767 (1999)

[9] A. Krimmel, A. Loidl, M. Klemm, S. Horn, D.V. Sheptyakov & P. Fischer, Physica B 350 e297–e299 (2004)

[10] H. Bakrima, K. Bouslykhane, M. Hamedoun, A. Hourmatallah & N. Benzakour, J. M. M. M. 327–334 (2005)

[11] H .Ishibashi, T. Y. Koo, Y. s. Hor, A. Borissov, Y. Horibe, P. G. Radaelli, S-W. Cheong, & V. Kiryukhin, Phys. Rev. B 66, 144424 (2002)

[12] Z. Szotek, W.M.Temmerman, A. Svane, L. Petit, P. Strange, G. M. Stocks, D. Kodderitzsch, W.Hergert & H. Winter, J. Phys.: Condens. Matter 16 (2004) S5587–S5600

[13]A. Krimmel, V. Tsurkan, D. Sheptyakov & A. Loidl, Physica B 378–380 583–584 (2006)

[14]Y. Kamihara, M. Matoba,T. Kyomen & M. Itoh, Physica B 1120–1121 (2006)

[15] P. G. Radaelli, Y. Horibe, M. J. Gutmann, & Hiroki Ishibashi, Nature, vol. 416 (2002).

[16] A. P. Ramirez & R. J. Cava, J.Krajewski, Nature (London) 386, 156 (1997)

[17] P. G.Radaelli, Y. Horibe, M. J. Gutmann, H.Ishibashi, C. H. Chen, R. M. Ibberson, Y.Koyama, Y-S. Hor, V. Kiryukhin & S-W. Cheong, Nature (London) 416, 155 (2002).

[18] K .Belakroum, thése de doctorat, université Mentouri-Constantine (Avril 2009)

[19] Y.C. Liao, C.H. Du, F. Xu, M.J. Wang, C. Wu, Y.Y. Hsu & M.K. Wu, Physica C 369–371 (2004)

[20] N. Buttgen et al., New J. Phys.61,191 (2004).

[21] R. W. Cahn & P. Haasen, E. J. Kramer –Materials Science and Technology- Vol.3B, Ed. VCH (1994).

[22] D. Schiferl & A. Waskowska. Phys. Rev. B 68, 094101 (2003).

[23]T. Hoshia, H. Aruga Katoria, M. Kosaka & H. Takagi, J. M. M. M, vol 310, e448-e450 (2007)

[24] H.A. Krug von Nidda, Habilitation, Université Augsburg (2007).

[25] M. Hemmida, these de magister, Université Augburg (2007)

[26] D. Mahl, J. Pickardt und B. Reuter, Z. anorg. Chem. 508 (1984) 197.

[27] D. Lou¨er, A. Boultif, Z. Kristallogr. Suppl. 23 (2006) 225.

[29] V. Tsurkan, V. Fritsch, J. Hemberger, H.-A. Krug von Nidda, N. B¨uttgen, D. Samusi, S. K¨orner, E.W. Scheidt, S. Horn, R. Tidecks, A. Loidl, J. Phys. Chem. Sol. 66 (2005) 2036.

[30] J. Krok,Kowalski, J. Warczewski, H. Duda, P. Gusin, K. Krajewski, T. ´ Sliwi´nska, A. Pacyna, T. Mydlarz, E. Malicka and A. Kita, Journal of Alloys and Compounds 430 (2007) 39.

[31] A. Abragam and B.Bleaney Electron paramagnetic resonance of transition ions. Oxford, England: Oxford University Press, 1970.

[32] M. Hamdoun, K. Bouslykhane, R. Masrour, F.Talbi, A.Hourmatallah and N. Bezakour. M. J.Condensed Matter 8 (2007) 1.

[33] E. Houze and M. Nechtschein, Phys. Rev. B 53 (1996) 14309.

[34] Z.Yang, X. Bao, S. Tan, and Y. Zhang, Phys. Rev B 69 (2004) 144407.

[35] M. Tovar, G. Alejandro, A. Butera, A. Caneiro, M. T. Causa, F. Prado, and R. D. Sanchez, Phys. Rev. B 60 (1999) 10199.

[36] G. Alejandro, M. C. G. Passeggi, D. Vega, C. A. Ramos, M. T. Causa, M. Tovar, and R. Senis, Phys. Rev. B 69 (2003) 214429.

[37] J. Deisenhofer, B. I. Kochelaev, E. Shilova, A. M. Balbashov, A. Loidl, and H.-A. Krug von Nidda Phys. Rev. B 68, (2003) 214427. 5

[38] E. Houze and M. Nechtschein, Phys. Rev. B 53 (1996) 14309

[39] Z.Yang, X. Bao, S. Tan, and Y. Zhang, Phys. Rev B 69 (2004) 144407

RESONANCE PARAMAGNETIQUE ELECTRONIQUE DANS LE COMPOSE SPINELLE CuCrZrSe4

Resumé : Nous rapportons sur les propriétés structurales et magnétiques de la CuCrZrS composés de spinelle e4. Méthode de Rietveld des diagrammes de diffraction des rayons X sur poudre révèle la structure spinelle normale AB2S e4, où les ions Cr3 + et Zr4 + occupent les sites B, tandis que le Cu1 + ions sont implantés sur un site. La susceptibilité magnétique une loi de Curie-Weiss supérieur à 250 K avec un ferromagnétique de Curie-Weiss température θp = 115 K et un paramagnétique instant μ_{eff} effective = 3.75μB par Cr3 + ion correspondant à la valeur de ag g = 1.94 en bon accord avec résonance de spin électronique (ESR) de mesures. En dessous de 100 K l'aimantation dévie du comportement de Curie-Weiss et se divise en champ refroidi (FC) et zerofield- refroidi (ZFC) branches. Une deuxième anomalie dans l'aimantation près de 10 K, qui est également visible dans les paramètres ESR, indique la transition dans un état de verre de spin en raison de la distribution aléatoire des ions Zr et Cr sur le site B. Cela est étayé par la dépendance en fréquence de l'anomalie détectée par des mesures de susceptibilité en courant alternatif.

Mots clés : Structure spinelle, Composé CuCrZrSe4, Dc et Ac, mesures magnétiques, spectroscopie ESR, comportement verre de spin

الرنين البارامغناطيسي الالكتروني في المركب السبيني CuCrZrSe4

الملخص: تم دراسة الخصائص البنيوية للمركب CuCrZrSe4 ذو سبين e4 بواسطة طريقة Rietveld على أساس بيانات حيود الأشعة السينية X وجد أن البنية السبينية من نوع AB2S e4 حيث الايونات Cr3 + و Zr4 + تشغل المواقع B بينما الأيونات Cu1 + تشغل المواقع A. القابلية المغناطيسة تحقق مبدأ Curie-Weiss أعلى من 250 كالفن و مغناطيسية حديدية الخاصة بدرجة حرارة Curie-Weiss p=250θ كالفن و العزم البارامغناطيسي الفعالμ_{eff}=3.75μB لكل أيون +*Cr*3 المقابل لقيمة g وأين g=1.94 حيث توافق تماما قياسات الرنين الالكتروني السبيني (ESR). تحت درجة حرارة 100كالفن, المغنطة تنحرف عن سلوك Curie-Weiss و تنقسم الى حقلين فرعيين :حقل مبرد (FC) وصفر حقل مبرد (ZFC). الشذوذ الثاني في المغنطة قرب درجة حرارة = 10كالفن والذي ايضا يكون واضح في معالم ESR ، يبين الانتقال الى حالة السبين زجاجي بسبب التوزيع العشوائي لأيونات Zr و Cr في الموقع B . و هذا ما يؤكده التردد المعتمد على الشذوذ المحقق عن طريق قياس قياسات القابلية AC .

الكلمات المفتاحية : البنية السبينية ، المركب CuCrZrSe4 ، القياسات المغناطيسية AC وDC ، التحليل الطيفي ESR ، سلوك سبين زجاج

Abstract : ELECTRON PARAMAGNETIC RESONANCE AND MAGNETIC SUSCEPTIBILITY IN THE CuCrZrSe4 SPINEL COMPOUND

Abstract:We report on structural and magnetic properties of the spinel compound *CuCrZrS e*4. Rietveld refinement of the powder x-ray diffraction patterns reveal the normal spinel structure *AB*2*S e*4, where the *Zr*4+ and *Cr*3+ ions occupy the *B* sites, while the *Cu*1+ ions are located on *A* sites. The magnetic susceptibility reveals a Curie-Weiss law above 250 K with a ferromagnetic Curie-Weiss temperature θ*p* = 115 K and an effective paramagnetic moment μ_{eff} = 3:75μ*B* per *Cr*3+ ion corresponding to a *g* value *g* = 1:94 in fair agreement with electron spin resonance (ESR) measurements. Below 100 K the magnetization deviates from the Curie-Weiss behaviour and splits into field-cooled (FC) and zerofield- cooled (ZFC) branches. A second anomaly in the magnetization close to 10 K, which is also visible in the ESR parameters, indicates the transition into a spin-glass state due to the random distribution of *Zr* and *Cr* ions on the *B* site. This is supported by the frequency dependence of the anomaly detected by AC susceptibility measurements.

Keywords: Spinel structure, CuCrZrSe4 compound, DC and AC magnetization measurements, ESR spectroscopy, Spin glass behaviour.